Published Online on 10 May 2016

Proc Indian Natn Sci Acad **82** No. 4 September 2016 pp. 1293-1301

DOI: 10.16943/ptinsa/2016/v82/48401

Research Paper

Rotary Entrainment in Stratified Gas-Liquid Layers: An Experimental Study

YAGYA SHARMA[1], PARMOD KUMAR[1], BASANTA K RANA[2] and ARUP K DAS[1,*]
[1]*Department of Mechanical and Industrial Engineering, IIT Roorkee 247 667, India*
[2]*Department of Mechanical Engineering, IIT Kharagpur 721 302, India*

(Received on 23 November 2015; Revised on 04 March 2016; Accepted on 16 March 2016)

Rotary entrainment is a phenomenon in which the interface of two immiscible fluids is subjected to external flux in the form of rotation. Present work reports the experimental study on rotary motion of a horizontal cylinder between the interface of air and water to observe the penetration of gas inside the liquid. Experiments have been performed to establish entrainment of air mass in water alongside the cylindrical surface. The movement of tracer and seeded particles has been tracked to determine the speed and path of the entrained air inside water. Simplified particle image velocimetry technique has been used to trace the movement of particles/tracers injected inside the entrainment zone and suspended beads have been used to replicate the particle movement with respect to time in order to determine the fluid flow dynamics along the cylinder. A thorough experimental analysis of air-water rotary entrainment phenomenon and its entrainment trajectories have been presented keeping in interest the extent to which these can be intermixed.

Keywords: Entrainment; Gas-liquid Flow; Particle Image Velocimetry; Stratified Layer Mixing

Introduction

The entrainment process can be related with several day to day life experiences such as gas-liquid reactors, aerated drinks, filling empty bottles etc. It is a complex and interesting phenomenon in which deformation of fluids takes place across the interface when subjected to some outside instability. This leads to heat and mass transfer between the interfaces of two immiscible fluids. It is also possible to have intermixing among the fluids by subjecting the interface to an external turbulent flux, which can subsequently lead to unbound advantages of intermixing of fluids. Rotary entrainment is a relatively new domain and exploitation of this phenomenon can lead to chemical reactions which were impossible to achieve due to their incapability of mixing together. Rotary entrainment is having plenty of applications in the field of oil and gas industries, chemical and petrochemical industry, pharmaceutical industry, gas-liquid chemical reactors, immiscible fluids chemical reactions and numerous others. The present study deals with the entrainment in the field of hydrodynamics which involve the movement of one fluid into another near the interface of two fluids. Specifically the rotary entrainment behaviour of two fluids with the help of a horizontal rotating cylinder between their interfaces has been experimentally investigated. Several research efforts have been made in this field over the past few decades. One of the earliest works done in this field used a rotating cylinder that is partially submerged in Newtonian fluid used a theoretical approach to determine the liquid flux picked up by a rotating cylinder and the variation of the film thickness around the periphery of the cylinder (Tharmalingam and Wilkinson, 1978). To predict thickness of the film, they assumed that a flat surface is withdrawn obliquely under laminar flow conditions from Newtonian fluids. Further, in a well presented series of work in this field was described the dependence of thickness of the liquid film carried upward by the surface of the cylinder to density ρ, viscosity μ and surface tension σ of the fluids (Campanella and Cerro, 1984). All the numerical and experimental results addressed in this paper were for

*Author for Correspondence: E-mail: akdasfme@iitr.ac.in

Newtonian fluids. In addition to the above, non-Newtonian fluids have also been considered with the horizontal rotating cylinder, which was partially submerged with a contact angle θ (Campanella *et al*., 1986). A film profile equation has been developed for a power-law type non-Newtonian fluid (Cerro and Scriven, 1980). This film profile equation allows computing a unique critical flow regime for each kind of power-law fluid. These fluids are characterized by two rheological constants mainly X and n, termed as flow consistency index and flow behavior index, respectively. Fluids having flow behavior index of one usually shows Newtonian behavior whereas fluids having n less than one are termed as Pseudoplastic and their counterpart is referred to as Dilatant. Pseudoplastic fluids usually have lower apparent viscosities at higher shear rates and show the dominance of shear thinning effect. However, the significant increase in viscosity of Dilatant fluids takes place at higher shear rates which make them prominent candidates for shear thickening. Film profile equation is based on theoretical understanding of the balance between viscous, gravitational and inertial forces, and presents the basic mechanisms for velocity profile development (Cerro and Scriven, 1980). They have also accounted the effect of capillary in the internal layers.The critical speed of the roller has been experimentally obtained by which entrainment of air has taken place along the sides of the roller (Bolton and Middleman, 1980). The formation of cusp like sharp structure on entrainment into the highly viscous pool on rotation solid roller partially submerged in the liquid pool. They have shown the functional dependence of width has been observed and the radius of curvature of sharp tip with the roller velocity scaled in terms of Capillary number (Lorenceau *et al*., 2003). The formation of two dimensional cusped interfaces at low has also been studied (Joseph *et al*., 1991) Reynolds numbers for both Newtonian and non-Newtonian fluids. Rotation of the partially submerged cylinder in the liquid has resulted in formation of cusp like structures. Generation of free surface cusps by the counter rotation of two parallel mounted cylinders on same horizontal plane below the free surface of viscous has been investigated for low Reynolds numbers (Jeong and Moffatt, 1992). The imposition of inertial, viscous, gravitational and surface tension forces has been on a liquid cylinder when it is being withdrawn from the liquid pool (Rebouillat *et al*. ,2002). A less relevant but similar study has predicted the thickness of liquid film on a vertically moving plate partially submerged in liquid, which has shown three regions of static meniscus, dynamic meniscus and constant film thickness during this upward motion (Spiers *et al*., 1974). All the studies presented till now are only with one liquid. However, the same technique could be employed to study viscous flow outside a horizontal rotating cylinder for two immiscible fluids. The experimental and theoretical analysis done on this system showed three regions of well-defined behaviour separated by two cataclysmic like transitions. While rotating a horizontal cylinder between two immiscible fluids these regions have been identified (Campanella and Cerro, 1986). These regions are:

a) Low removal velocities: A dynamic contact line on the cylindrical surface is observed between the two fluid regions. This velocity regime is observed on the top of the cylinder which was coated with the lighter fluid.

b) Intermediate removal velocities: The moving contact line that is detected in the low removal velocities disappeared and it is sucked up by the movement of the solid surface. The cylindrical surface in this region is coated with both the fluids.

c) Large removal velocities: The lighter fluid layer could not approach the surface of the cylinder and the bottom of the cylinder is the only coated with heavier fluid.

The film thickness around a horizontal rotating cylinder numerically has been estimated using the volume of fluid (VOF) method to clarify the film-formation process around the rotating cylinder (Yu *et al*., 2009). Parametric studies have been performed to compare the effects of ink properties (viscosity, surface tension) and operational conditions (roller rotational speed, initial immersed angle) on film thickness. Viscosity and rotational speed of the cylinder played a dominant role in determining the thickness of the film.

Sufficient experimental, numerical and theoretical research has been done till date, to determine the flow rate and thickness of the film which develops due to the rotation of the cylinder. However,

entrainment between air-water interfaces has not been investigated in detail. All the work mentioned before have been used to expound the coating process. Moreover, its utilization in mixing of a two phase fluid has yet not been exploited. Besides, work has still not been done to calculate the height or the distance from the interface to the zone up to which entrainment phenomenon is experienced. The film that has been mentioned in the references is basically the entrainment zone which occurs due to drag force applied by the cylinder on the viscous fluids. In this study, an attempt has been done to determine the flow of this entrainment zone using ink dispersion technique, particle image velocimetry and particle tracking velocimetry. All the above mentioned phenomena have been captured to understand the flow dynamics of fluid-fluid entrainment. A theoretical formulation has been performed to understand the process that occurs on subjecting the interface to an external flux with the help of rotating cylinder.

Experimental Details

Design of Experiments

A 50 x 50 x 50 cm^3 cubical container made of Perspex sheet is used to build the exterior of the setup. The cubical container is left open at the top, to facilitate easy addition and removal of the fluid. A 30 cm long cylinder of radius 3 cm is mounted on a shaft and fixed along its horizontal axis at the two opposite sides of the container at 25 cm height from the bottom. Warm wheel is mounted on the one end of shaft which engages with its counterpart, which is connected to the drive shaft. Another end of the drive shaft is coupled to a variable speed DC motor which is fixed to the top of container surface. The maximum rated rpm of the motor is 5000 and the speed ratio of gear assembly between the two shafts is 25. To prevent leakage of fluid from the container, washers have been used to air tight the ends of the shaft. Regulated DC power supply unit gives the reading in the form of voltage and current with its output ranging from 0-13.4 V DC and 20 A maximum current. The input of this power unit is given a supply line voltage of 230 V AC, 50 Hz. Desirable speed of the cylindrical roller is obtained by varying the rpm of the motor using a knob mounted in power supply to regulate the supply voltage. A high speed camera (Make: Ximea) has been employed with 500 frames per second to capture the experimental phenomenon at 1856 x 1548 pixels. Another digital camera with 25 frames per second has also been used to capture the phenomenon with a frame width of 1440 pixels and frame height of 1080 pixels. The former is referred to as Camera A and later one is referred to as Camera B in the subsequent text. To facilitate proper lighting two halogens of 500 W (with reflector and heat resistant glass in front) each is engaged on opposite ends of the container. As the setup has been built of Perspex sheet, it is transparent on all sides to facilitate easy observation of the phenomenon. Digital image processing is performed on the captured images. A schematic of the test facility is shown in Fig. 1.

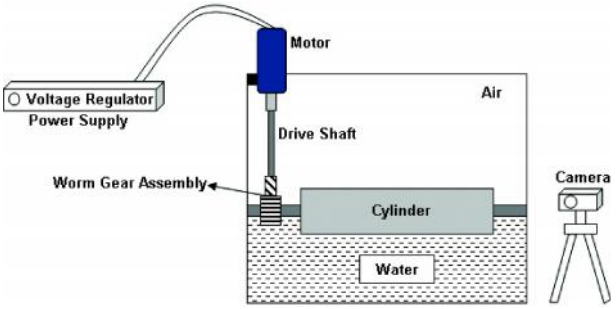

Fig. 1: Schematic of experimental setup

Methodologies

To consolidate the experimental findings on entrainment three different procedures have been used. Initially, the test section is half filled with water and DC motor is fixed to the drive shaft. The desired rating of the motor is obtained by adjusting the output voltage of the power supply. Clearly defined entrainment phenomenon has been observed on rotations of the rotor between air and water interface. To elaborate on this observation, several techniques have been used to determine the flow dynamics/ trajectories of the entrainment.

One of the methods that have been employed is ink dispersion technique. Ink is explicitly injected through a volumetric pipette to introduce very precise and trivial volume of ink to the water surface near the entrainment zone. The flow of the ink has been observed and captured with the help of Camera B. Further to track the velocity vectors of particles inside the entrainment region, Particle Image Velocimetry

(PIV) method has been used. In this method, the fluid is seeded with tracer particles. The fluid with entrained particles is observed and the motion of the seeded particles is used to calculate the velocity field of the flow under study. During the use of PIV technique, the particle concentration is adjusted in a manner to identify individual particles in an image. The seeding of particles is an inherently critical component of the PIV system. Depending on the fluid under investigation, the particles must be able to match the fluid properties reasonably well. Otherwise they will not follow the flow satisfactorily enough for the PIV analysis to be considered accurate. Hence, the best suited spherical shaped golden glitter particles with average diameter of 0.02 mm have been used to capture the present phenomenon. 12 ml solution of water and glitter particles at a concentration of 20-25% is injected into the entrainment zone at constant rate with the help of a funnel having 3.8 mm outlet diameter. The zone of investigations is limited within a distance of 10 mm from the cylinder surface for PIV analysis. Particle trajectories have been observed by splitting the captured videos into corresponding frames at successive times. Minimum three videos are taken for each PIV investigation and averaged values of all parameter are obtained for further analysis. However, to track individual particles, Particle Tracking Velocimetry (PTV) method has been used. It is a technique to measure velocity of particles dropped inside the fluid. While PIV technique is an Eulerian method approach, though PTV can track individual particles and follow Lagrangian approach. Golden colored spherical shaped aluminium particles with an average diameter of 2.5 mm have been used as the seeding particles to track velocity field in the entrainment region. The particles are seeded in the entrainment region under the action of gravitation pool with the help of 3 mm internal diameter glass tube. Number of particles seeded varies in between five to seven, while the path of three particles is tracked during the analysis. Particles are seeded at three different equally spaced locations within a distance of 5 to 10 mm from the cylinder surface with almost zero height of injection from the air-water interface in order to avoid the effect of initial particle acceleration.

Results and discussions

Rotary Entrainment

Rotary entrainment phenomenon is observed at 200 rpm between air-water interface. A distinct protuberance of water is visible in the air medium indirection of rotation of cylinder, whereas a dip is found on the opposite side of the cylinder along its longitudinal axis. Fig. 2 depicts the cylinder rotating in clockwise direction with a water protrusion in the air medium and a dip in the water due the entrance of air mass.

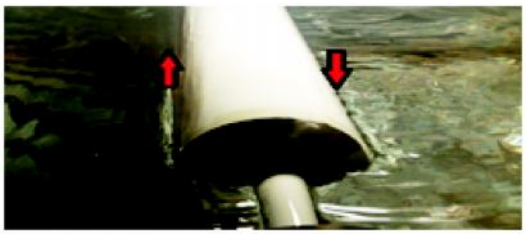

Fig. 2: Rotary Entrainment: formation of water chute and air chute

Fig. 3 shows the entrance of water in the air medium. This protuberance of a film of fluid in another medium is called chute. In this case it is the water chute entraining in the air medium. Fig. 3 depicts the front view of the test facility in which a clear indication of water chute is observed entering in the air medium along the direction of rotation of the cylinder.

Fig. 3: Water chute in air medium

Ink Dispersion Technique

To determine the flow dynamics of the entrainment, a minuscule drop of ink is injected near the entrainment region and the cylinder is rotated at three different speeds of 50, 115 and 185 rpm. Video is captured with the help of Camera B from the time the water is pigmented with the ink to the time it disperses in the

water. The video is then split into frames to observe the ink flow. The region of air chute formation in the entrainment region where ink is injected; is shown in Fig. 4.

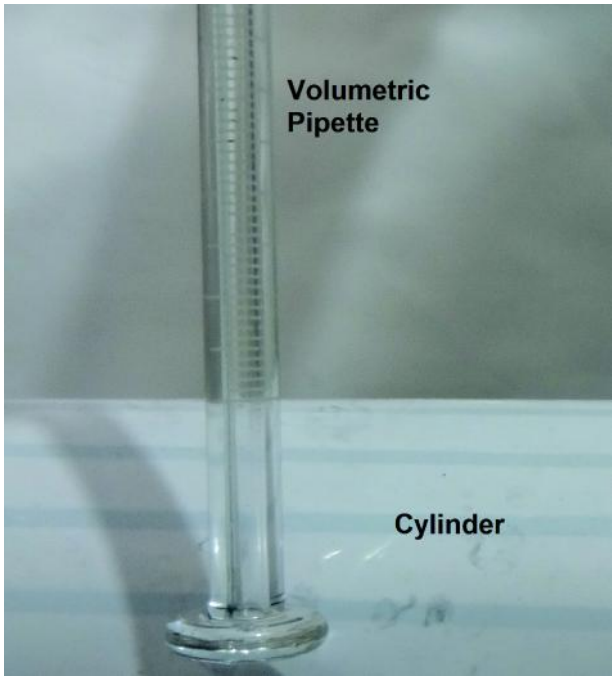

Fig. 4: Injection of ink in entrainment region

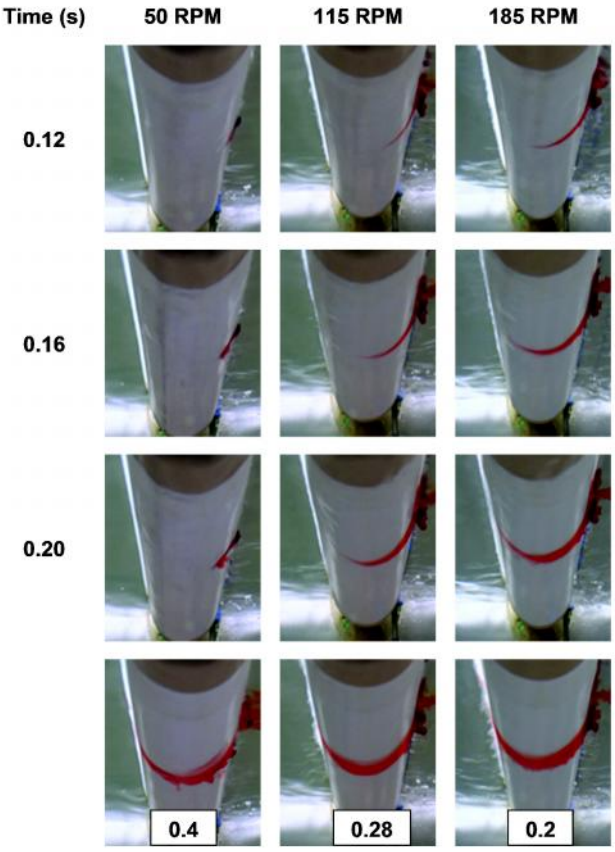

Fig. 5: Flow of pigmentation under influence of entrainment

It is observed that the ink immediately flows to the region where dip has formed due to the rotation of cylinder. This gives a clear indication of a pressure difference prevalent at the same level in the container. This leads to the conclusion that an altered region is present near the cylinder that has properties different from rest of the water medium. Further, the ink follows a specific path covering approximately one fifth of the circumference of the cylinder before getting dispersed at low rpm. However, the periphery of this sharp ink water interface has increases with increase in speed of the cylinder. The discrete path followed by the ink could be associated to the fact that the entrainment region of air has its effect inside the water, only till the point where the ink starts to disperse as presented in Fig. 5. This reveals the fact that periphery of the entrainment region increases with increase in speed of cylinder, as shown in Fig. 5 for three different speeds.

The images have been discretised and analysed with the help of a scripted code. The tip of the ink is tracked in each picture. Distance and the angle made by the tip of the ink have been measured from the centre of the cylinder. These have been used to calculate the tangential, radial and total velocity using eqn. (1), where ν is the total velocity vector, *r(t)* is the radial distance of ink tip from the centre of the cylinder with time and α is the angle made by the ink tip from the centre of the cylinder. An indigenous code has been scripted to analyze the data and determine the velocity vectors for different time stamps

$$\nu = \frac{r(t)}{dt} = \frac{dR}{dt}\alpha + \frac{Rd\alpha}{dt} \tag{1}$$

It has been seen that tip of the ink has moved along the cylinder surface only so there exists no gradient in radial direction with time. Hence, the magnitude of the radial velocity is almost zero for the present experiments. Angular variation of ink tip is plotted against the time in Fig. 6 for three different rotational speeds of the cylinder. It is observed that the angle of the ink tip has increased at higher rates

for high cylinder rpm. This variation is obvious due to the presence of deeper entrainment regions for the high rotational speeds. As soon as it ends, the ink starts diffusing in the water. The inset of Fig. 6 also shows the variation of ink tip tangential velocity with time. An initial rise in tangential velocity is seen for the high rotational speeds which are subsequently followed by the decrease in velocity. However, there is no such initial pickup for the ink tip when cylinder is rotated at 50 rpm. The point at which the ink starts to disperse is the point of maximum velocity and it is the end of air chute. Once ink reaches the dip, the velocity-time graph assumes an increasing slope till the point chute reaches its maximum height. After which the graph assumes a decreasing slope and this is the point where ink starts to disperse and effect of entrainment ends.

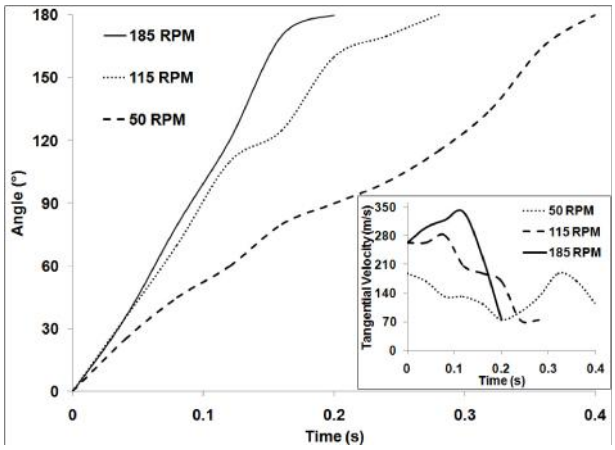

Fig.6: Variation of ink tip angles and tangential velocities with time

Particle Image Velocimetry (PIV)

The entrainment phenomenon has been captured at 300 rpm of the cylinder. Golden glitter particles have been dropped with the help of funnel under the influence of gravity just near the entrainment region. It is witnessed that the glitter particles follow a discrete path just near the cylindrical surface. The particles follow the flow around the cylinder for about one-fifth of the cylinder's circumference. It is observed that in this region the particles are present in large density and they all move along the cylinder due to the presence of air chute in water. However, once the influence of the air chute diminishes, the particles tend to fall under the influence of gravity. Hence, it can be stated that entrainment phenomenon makes its presence felt inside water only up to a certain depth. However, it is observed that some of the particles are able to traverse the whole cylindrical surface immersed inside the water medium. This occurrence is due to the pull force associated with the water chute formation in air medium. The flow dynamics of glitter particles is shown in Fig. 7, which has been captured using Camera A. The depth till which air chute can entrain in the water is dependent on the rpm of the cylinder and the physical properties of the two fluids.

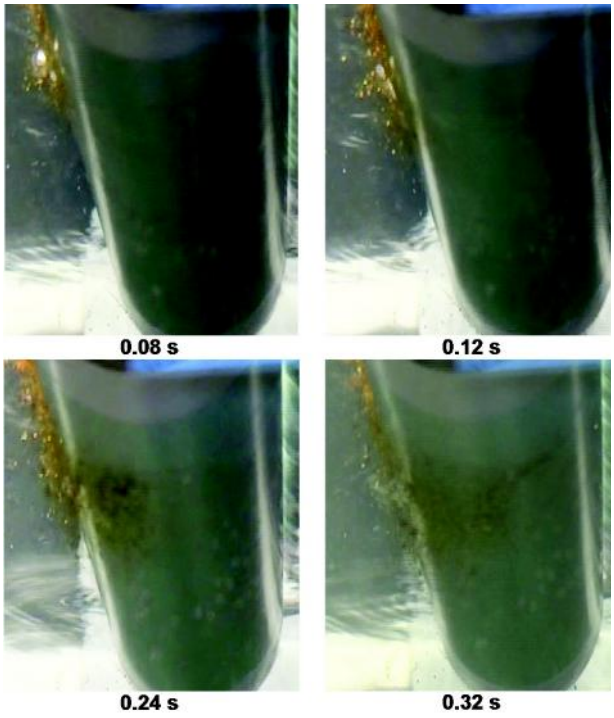

Fig. 7: Flow of seeded particles at different time stamps

Particle Tracking Velocimetry (PTV)

The cylinder is rotated at 275 rpm in the air water interface to track entrainment velocities. Each bead is dropped at a different distance from the air chute. However, it is observed that soon they trace their path towards the entrainment dip and then follow a path alongside the cylinder up to a certain point. This occurrence has been captured with the help of Camera A. The paths followed by the beads have been determined by splitting the videos captured by the camera into frames. Each image has been analysed with the help of a scripted code. Three bead particles

are tracked and their distances and angles made from the centre of the cylinder in the images have been recorded with respect to time. Velocity of each bead has been calculated using an in-house code scripted to find out the radial, tangential and total velocity of the beads by using eqn. (2), where *u* is the total velocity vector of the bead, *R(t)* is the radial distance of the bead from the centre of the cylinder with time and β is the angle made by the bead from the centre of the cylinder. The total velocity vector has been plotted against time for the three beads. Fig. 8 shows comparison among the total velocity vectors of the three beads dropped at different distances of 0.5 cm, 0.75 cm, 1 cm away from the cylinder with respect to time, respectively

$$u = d\frac{R(t)}{dt} = \frac{dR}{dt}\beta + \frac{Rd\beta}{dt} \tag{2}$$

After the beads fall on the water surface at 0.5cm, 0.75cm and 1cm from the entrainment zone, it is observed that the bead nearest to the cylindrical surface has the highest initial velocity and the bead farthest from the cylinder has the lowest initial velocity. The velocity of the beads decreases up till the point they enter the entrainment zone near the surface of the cylinder. However, as soon as they enter the chute, their velocity starts to increase and reaches a maximum value at around 0.6 seconds for the observed data. These maxima are the end of the area under the effect of air chutes in water. After that the speed decreases and some of the beads drop under the influence of gravity as the effect of entrainment becomes negligible in that region. Nevertheless, the particles that continue to move along the cylinder again experience an increase in their velocity as they enter the water chute region on the other side of the cylinder. Once the beads reach the apex of the water chute, they reach their maximum velocity before drifting back in the water medium with a decrease in velocity. We observed a very high velocity of all the beads when it is just entering in the pool and then its velocity becomes steady. Initially the bead near to the surface gets higher velocity due to inertia in the cylinder. Away from the cylinder the induced velocity reduces due to viscous effect of the liquid.

Relation between RPM, Entrainment Depth and Radius of Curvature

After finding out the results related to the flow

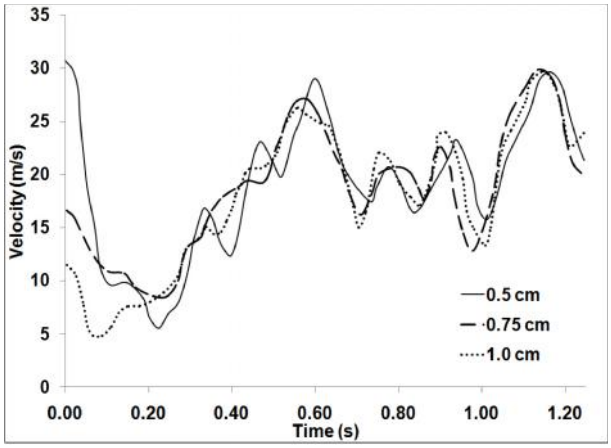

Fig. 8: Total velocity-time graph for different beads dropped at 0.5 cm, 0.75 cm and 1 cm from the cylinder surface, respectively

dynamics of the entrainment region, an indigenous code is scripted to note the changes observed in the entrainment zone with respect to change in the rpm of the rotating cylinder. The cylinder is run at three different rotational speeds, 165, 200 and 245 rpm. It is visually observed that with increase in velocity of cylinder the penetration of the air-water entrainment zone increases in the nearby region around the cylinder. Hence, two parameters, radius of curvature and maximum depth of entrainment have been taken to represent the physical properties of the entrainment. Videos have been captured using Camera A and has been later analysed frame by frame using an indigenous code to observe the entrainment of air chute inside water at different rpm. To quanitfy the visually observed results, a code is written to capture the pixels of the images near the entrainment region and edge detection technique has been used to obtain the shape of the air chute. For a specefic rpm, few images are selected to obtain the time-average curve of the entrainment. From the curve, the depth of the air chutes for different rpm have been obtained. The depth is representative of the fact that the effect of the air chute inside water is only up to this height. Furthermore, another code has been scripted to find out the radius of curvature of the curve using the points obtained from previous code. The interface of the entrainment region for different cylinder speeds has been plotted in Fig. 9.

It is observed that with increase in the rotational speed of the cylinder, the radius of curvature as well

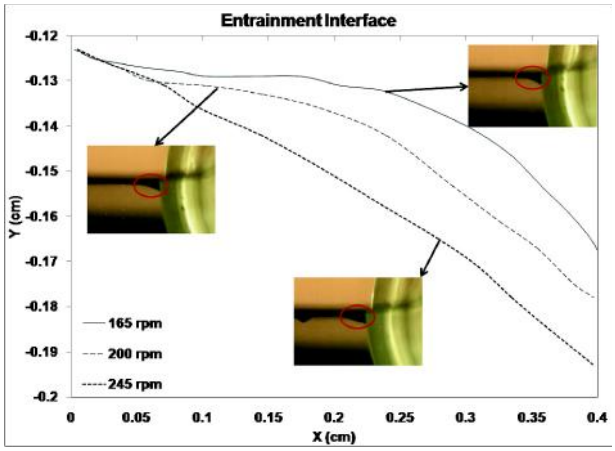

Fig. 9: Interface of entrainment and its depth for different rpm

as the depth of the entrainment increases. That is, the curve starts to become flatter and at the same point the tip of the entrainment zone extends to a deeper region inside water. Fig. 10 shows the variation of radius of curvature and depth of penetration for respective cylinder speeds.

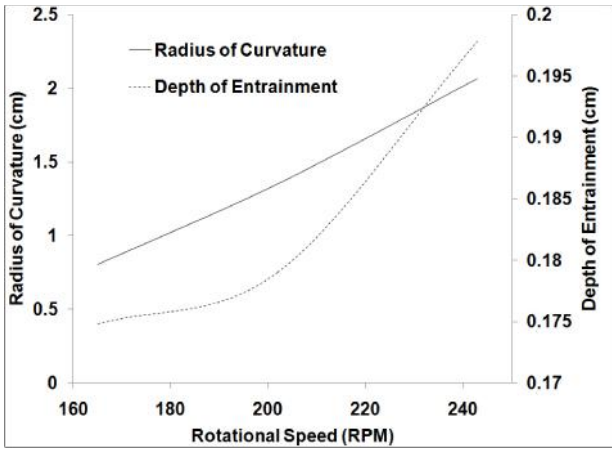

Fig. 10: Variation of radius of curvature and depth of entrainment with rotational speed of the cylinder

Conclusion

An effort has been made to study the rotary entrainment in water-air interface by a half-submerged cylinder which is rotated at different speeds. To estimate the air entrainment zone different techniques have been employed, such as ink dispersion technique, Particle Image Velocimetry and Particle Tracking Velocimetry. Variation of tangential velocity of ink tips and golden beads with time have been estimated in detail with different position of impact. The depth of penetration as well as the radius of curvature of air entrainment has been found for different roller rotational speed of half submerged cylinder. It is established that when a cylinder is rotated on the interface of two fluids, an entrainment zone is formed. This entrainment zone is in the form of a dip in the direction of rotation of cylinder. The findings also establish that the tip of the entrainment zone has the maximum velocity. Moreover, it is also established that with an increase in the rotational speed of the cylinder, the radius of curvature of the chute as well as the depth of entrainment of the zone increases.

Acknowledgement

AKD wishes to acknowledge support of IIT,Roorkee through Faculty Initiation grant. YS, PK and BKR want to thank IIT, Kharagpur for support in providing high speed camera.

Nomenclature

ρ	Density [kg/m^3]
θ	Angle of contact [rad]
μ	Viscosity [N-s/m^2]
σ	Surface tension [N/m]
R	Radius of cylinder [m]
X	Flow consistency index [Pa-s^n]
n	Flow behavior index
ν	Total velocity vector of ink [m/s]
α	Contact angle of ink [rad]
r(t)	Radial distance of ink [m]
u	Total velocity vector of bead [m/s]
β	Contact angle of bead [rad]
R(t)	Radial distance of bead [m]

References

Bolton B and Middleman S (1980) Air entrainment in a roll coating system *Chemical Engineering Science* **35** 597-602

Campanella O H and Cerro R L (1984) Viscous flow on the outside of a horizontal rotating cylinder: The roll coating regime with a single fluid *Chemical Engineering Science* **39** 1443-1449

Campanella O H, Galazzo J L and Cerro R L (1986) Viscous flow on the outside of a horizontal rotating cylinder-II. Dip coating with a Non-Newtonian fluid *Chemical Engineering Science* **41** 2707-2713

Campanella O H and Cerro R L (1986) Viscous flow on the outside of a horizontal rotating cylinder-III. Selective coating of two immiscible fluids *Chemical Engineering Science* **41** 2713-2721

Cerro R L and Scriven L E (1980) Rapid free surface flows: an integral approach *Industrial and Engineering Chemistry Fundamentals* **19** 40-50

Jeong J T and Moffatt H K (1992) Free-surface cusps associated with flow at low Reynolds number *Journal of Fluid Mechanics* **241** 1-22

Joseph D D, Nelson J, Renardy M and Renardy Y (1991) Two-dimensional cusped interfaces *Journal of Fluid Mechanics* **223** 383-409

Lorenceau E, Restagno F and Quere D (2003) Fracture of a viscous liquid *Physical Review Letters* **90** 184501 1-4

Rebouillat S, Steffenino B and Salvador B (2002) Hydrodynamics of high-speed fibre impregnation: the fluid layer formation from the meniscus region *Chemical Engineering Science* **57** 2953-3966

Spiers R P, Subbaraman C V and Wilkinson W L (1974) Free coating of a Newtonian liquid onto a vertical surface *Chemical Engineering Science* **29** 389-396

Tharmalingam S and Wilkinson W L (1978) The coating of Newtonian liquids onto a rotating roll *Chemical Engineering Science* **33** 1481-1487

Yu S H, Lee K S and Yook S J (2009) Film flow around a fast rotating roller *International Journal of Heat and Fluid Flow* **30** 796-803.